

RGB-based Semantic Segmentation Using Self-Supervised Depth Pre-Training

Jean Lahoud, Bernard Ghanem

King Abdullah University of Science and Technology (KAUST)

Thuwal, Saudi Arabia

{jean.lahoud,bernard.ghanem}@kaust.edu.sa

Abstract

Although well-known large-scale datasets, such as ImageNet [8], have driven image understanding forward, most of these datasets require extensive manual annotation and are thus not easily scalable. This limits the advancement of image understanding techniques. The impact of these large-scale datasets can be observed in almost every vision task and technique in the form of pre-training for initialization. In this work, we propose an easily scalable and self-supervised technique that can be used to pre-train any semantic RGB segmentation method. In particular, our pre-training approach makes use of automatically generated labels that can be obtained using depth sensors. These labels, denoted by HN-labels, represent different height and normal patches, which allow mining of local semantic information that is useful in the task of semantic RGB segmentation. We show how our proposed self-supervised pre-training with HN-labels can be used to replace ImageNet pre-training, while using 25x less images and without requiring any manual labeling. We pre-train a semantic segmentation network with our HN-labels, which resembles our final task more than pre-training on a less related task, e.g. classification with ImageNet. We evaluate on two datasets (NYUv2 [28] and CamVid [3]), and we show how the similarity in tasks is advantageous not only in speeding up the pre-training process, but also in achieving better final semantic segmentation accuracy than ImageNet pre-training.

1. Introduction

One of the main goals in computer vision is to achieve a human-like understanding of images. This understanding has been recently represented in various forms, including image classification, object detection, semantic segmentation, among many others. All of these tasks are alleviated with large annotated datasets, especially after the emergence of deep learning techniques. The importance of such large-scale datasets e.g. ImageNet [8], can be easily ob-

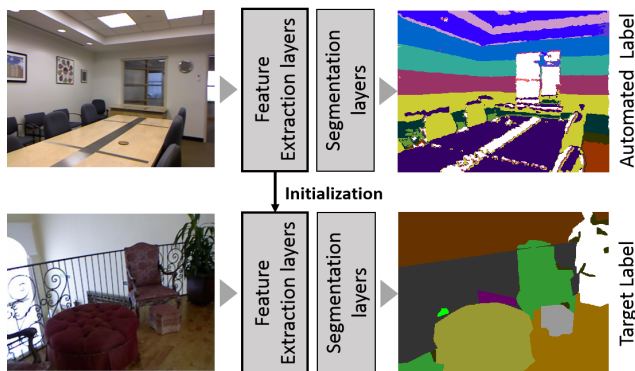


Figure 1. **Self-supervised learning with depth for pre-training.** Typically, a semantic segmentation model is initialized using another model pre-trained using hand labelled images (e.g. ImageNet). We propose HN-labels that can be automatically generated from corresponding depth maps. These labels can be used for pre-training while maintaining the final semantic segmentation performance.

served in most deep learning methods, as nearly all techniques initialize from models pre-trained on these datasets.

Since annotation is tedious and cannot be easily scaled, it currently represents a bottleneck to the advancement of deep learning methods. In an attempt to address this limitation, several approaches have explored the potential to minimize the amount of manual work required prior to training. One of the main trends today is the use of synthetic datasets to create photo-realistic environments that are inherently labeled. Although synthetic images have become to some extent similar to images taken in real environments, generating these realistic-looking scenes still requires considerable manual effort in most cases. Another promising research direction is self-supervised learning, as well as reinforcement learning. Such learning does not require annotated data, and hence loosens the tie between learning methods and available datasets. Nevertheless, these techniques require correct modeling and might become computationally demanding.

This work aims at generating labels that (i) can be auto-

Method Requirement	Scalability	Straightforward Modeling	Data Available at test	Transferable to RGB only
Labeled RGB	–	++	++	++
Labeled RGBD	–	+	–	–
Synthetic	o	++	++	o
Self-supervised	++	–	++	++
Model Based	–	o	–	o
Ours	+	++	++	++

Table 1. **A comparison between various training requirements for semantic segmentation.** We show the advantages (+) of every method requirement as well as the disadvantages (–). (o) implies unclear benefit to the corresponding specification. Our proposed method is easily scalable, and operates directly on RGB images at test time without the need for additional information. Model based methods require a library of known shapes, such as 3D CAD models.

matically obtained without manual annotation, and (ii) improve the task of semantic segmentation. Specifically, we use the depth channel supplied by RGBD sensors to extract patches that are labeled according to height and normal information only. We denote our labels by HN-labels, which we use to pre-train a semantic segmentation network in a self-supervised fashion. In this way, both our pre-training and training processes are closely related as both aim at semantically segmenting a given scene. Our method makes use of this depth information for pre-training only, as depth information need not be present at inference time.

We show how our HN-labels can easily replace large-scale annotations required for pre-training. An added advantage of our proposed technique is that it helps introduce new segmentation models not based on popular architectures such as VGG-16 [33], AlexNet [23], GoogleNet [35], and ResNet [18]. Our goal is to substantially reduce the amount of manual work required prior to training. Therefore, we formulate the pre-training as a self-supervised learning process. The only manual work needed is the collection of aligned RGBD images, which is straightforward, not time consuming, and does not require manual semantic labeling. Figure 1 shows the end target of our method: to replace hand-labeled datasets used in initializing semantic segmentation networks with a dataset that can be easily collected and automatically labeled, without significant impact to segmentation performance.

We formulate the initialization as an HN-labels segmentation task, which is closely related to semantic segmentation. The HN-labels represent different classes that are automatically formed based on grouping normal angles and height relative to the floor plane. Learning to segment the HN-labels classes enables mining of local semantic information. We show how initializing from a closely related task is much more efficient than initializing from less related tasks. Predicting heights and normals from a single RGB image is a by-product of our method and is not the main goal. Similar to depth estimation, height can take continuous values in 3D which makes the estimation task harder. Nevertheless, indoor scenes usually have structured

environments in which common objects generally have similar heights. Unlike depth, it is important to note that height are independent of the camera viewpoint.

Table 1 shows a comparison between the various training requirements of semantic segmentation techniques. Our approach aims at providing labels that can be easily scaled, do not require additional complex modeling, and can be easily used to label any given RGB image.

2. Related Work

Since this work aims at providing better semantic segmentation based on transferring knowledge from a closely related and easily scalable self-supervised task, we provide a literature review on three related topics: (i) semantic segmentation, (ii) multi-task and transfer learning, and (iii) self-supervised and scalable learning.

Semantic Segmentation: The recent success of deep learning techniques in image classification and object detection have motivated researchers to explore the task of semantic segmentation with deep learning. This could only be achieved with pixel-level labeling provided by large-scale datasets, such as PASCAL VOC [10], MS COCO [25], Cityscapes [7], CamVid [4], and KITTI [12]. Most recent methods benefit from existing classification CNNs (Convolution Neural Networks) by adapting them into ones that can output pixel labeling instead of classification scores. An early method is the Fully Convolution Network (FCN) network [26], which replaced the fully connected layers of popular classification networks with what was later referred to as ‘deconvolutions’ to produce pixel labeling. A similar approach was proposed with the SegNet architecture [2], which also utilized convolution layers from a classification network (encoder), but introduced a different up-sampling mapping (decoder). The up-sampling was done through multi-stage learnable ‘deconvolutions’ with up-sampling indexed similar to max-pooling indices of the encoder part. These techniques, along with numerous others such as [5, 6, 39, 37], require large-scale datasets in training and can only be improved with more groundtruth labeling.

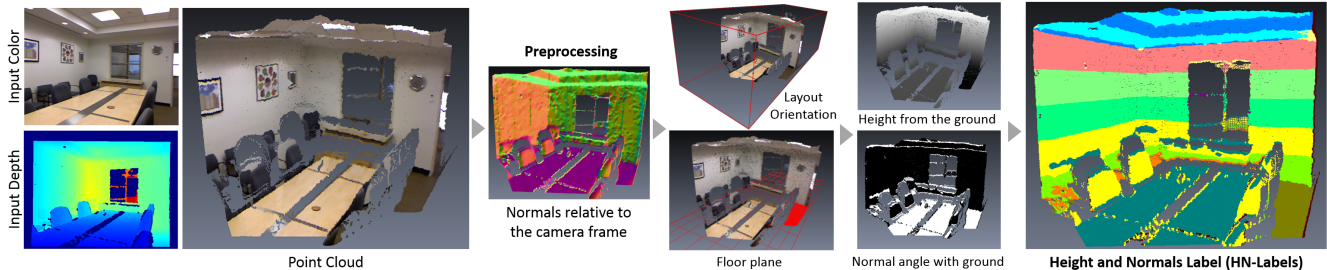


Figure 2. **General overview of our method.** Given an RGB image along with its corresponding depth image, we compute the normals on the generated point cloud. We then estimate the room orientation, and extract the floor plane. Height and normal angles relative to the floor are then used to generate our HN-labels.

Indoor scenes benefit from the use of off-the-shelf RGBD sensors that measure coupled depth and color information. Multiple datasets were collected using such sensors and were labeled for pixel-level semantic segmentation, including NYU-D v2 [28] and SUNRGBD [34]. Encoding the depth cue as an input to neural networks is not straightforward, and multiple approaches have been proposed. Gupta *et al.* [16] proposed to encode depth as additional channels in the form of horizontal disparity, height above ground, and the angle between the local surface normal and the gravity direction (HHA). This leads to better segmentation compared to using the color channel alone. However, this method, similar to all RGBD-based techniques, requires the presence of depth information at inference time.

Transfer Learning and Multi-task Learning: In practice, most CNN approaches do not train their models from scratch. Instead, learned feature extractors are transferred [32] from models trained on large-scale datasets, such as ImageNet [8]. Other forms of transfer learning can be done by pre-training on synthetic datasets [30, 11]. Transfer learning can be viewed as a special case of multi-task learning, where tasks are sequentially learned instead of being jointly learned. Numerous works train a network to perform multiple tasks simultaneously. The approach proposed by [9] jointly predicts depth, surface normals, and semantic labels with a multi-scale network. Although these tasks are closely related, labels for all tasks need to be available for training. The work presented in [27] introduces a principled way to share activations from multiple networks. The sharing unit, known as cross-stitch, can be trained end-to-end to choose between sharing the layers or separating them at task-specific activations. Other work [21] proposes a systematic way to combine multiple loss functions of multiple tasks by considering the uncertainty of each task.

Self-Supervised Learning: The technique presented in [38] proposes a self-supervised method to generate a large labeled dataset without the need for manual labeling. Labels of known objects were generated by manipulating the camera around a controlled environment, in which object

locations are known. The generated dataset was then used to train a robot to better perform in picking tasks. A main drawback of this technique is that the dataset was generated in a controlled environment with known camera locations and also required human involvement in arranging objects. Other self-supervised techniques aim at regressing depth from videos [14, 40, 36]. Hence, these techniques are good at estimating depth especially in outdoor scenes in the context of autonomous driving. These applications mainly focus on objects located on the road. This greatly differs from how objects are arranged in indoor scenes. Since we model our pre-training as a self-supervised process, the amount of RGBD data that is available for pre-training is large and can be easily scaled up. One can easily append training data with personal data collected with RGBD sensors in any environment of interest. Self-supervision for representation learning was also explored in [29, 24], in which proxy tasks were proposed using the color images. Although our proposed proxy segmentation task requires depth data, this additional data provides information that cannot be learned from the image alone. Techniques, which only require color, are a good alternative, but since they are not provided with inaccessible information, their performance is shy of ImageNet pre-training for the same task.

Contributions. We propose a self-supervised technique for the task of height and normal estimation from a single RGB image. The network trained on this task can be used to initialize a semantic segmentation network. We show how this self-supervised pre-training strategy can be easily scaled and is more efficient than initializing from networks trained on different fully supervised tasks. Our experiments show that semantic networks initialized using our proposed self-supervised method outperform ones initialized from networks trained on large-scale datasets annotated for a different task.

3. Methodology

Our method aims at overcoming the limitations of semantic segmentation techniques when training on a small

dataset or when training from scratch. An overview of our method is depicted in Figure 2. In the following sections, we detail our process in choosing the labels, generating the dataset, and using these labels to pre-train a given network.

3.1. Alternative Category Representation

The motivation to this work is to look at the depth channel as a source for labeling RGB images. RGBD sensors are used to easily collect aligned color and depth image pairs. Our aim is to automatically generate labels that are not necessarily designed for the target task (semantic segmentation), but could afford helpful information for it. Successfully transforming depth into labels makes this method capable of generating *free* labels as compared to the tedious, time consuming, RGB pixel labeling needed for semantic segmentation. The first intuitive use of depth is to train a network to directly regress the depth from a single RGB image. However, depth requires complex knowledge of the environment and varies with camera location/viewpoint.

With the complexity of indoor scenes, regressing depth necessitates a high capacity network and can be tedious to train. On the other hand, with additional effort, one can transform depth into height above ground, which is view-independent. Taking the ground plane as reference, one can also transform normals relative to the camera viewpoint, which depend on camera angle, to view-independent normal angles relative to the ground plane.

Our method uses height and normal information as the main precursor for pre-training. We choose to bin the height into n_h bins (or levels) and normals into n_n bins and train a model to output the correct normal and height level per pixel. Since it learns to generate features specific to segmentation, this pre-training is closer to our end goal of semantic segmentation than to pre-train with models trained on other tasks, *e.g.* image classification. In fact, one can think of height bins as semantic segmentation with object part specific labels: chair and table lower legs, lower part of wall and door, table top, and sofa back, *etc.* This type of grouping consistently clusters objects and their parts into specific bins. To highlight this point, Figure 3 shows the height distribution of 40 indoor objects on a subset of NYUv2 dataset [28]. For every object, we show the percentage of its occurrence in every height bin. As expected, objects like floor (label 2) and floor mat (label 20) only occur within the lowest height bin, whereas ceiling (label 22) occurs within the highest bins. Other objects almost always occur in the same bin, such as bathtub (label 36) and counter (label 12). Furthermore, when considering other object classes, there exists an overall trend in height, with object parts falling in specific height bins. In light of these observations, training a network to distinguish between different height levels will inherently train it to distinguish between some object classes and/or their parts. This informa-

tion is expected to be useful for the task of semantic segmentation.

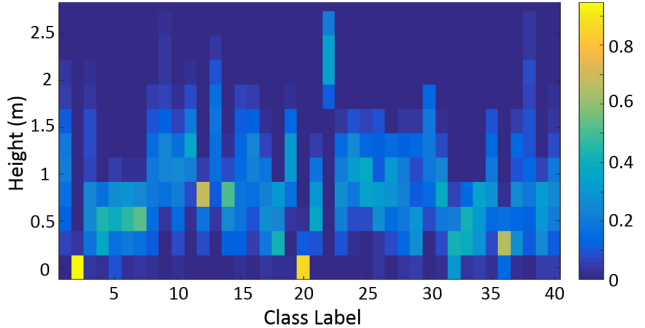


Figure 3. **Object height distribution.** This colormap shows the distribution of height for various object classes in NYUv2 [28]. Colors represent the fraction of 3D points of the same label that are located at a particular height bin.

3.2. Automated Label Collection

Floor Identification: Our method mainly relies on the floor plane as a reference for the proposed labels. To identify a possible floor plane, we first use the camera intrinsic parameters to map the depth image into a 3D point cloud. Next, we compute the normals at each 3D point using the method of [31]. We then use the normals to estimate the scene layout orientation using the method of [13]. Once the orientation is obtained, the room is rotated to make the ground normal aligned with the upward direction. Afterwards, we choose the ground location as the first percentile of points along the upward direction. The first percentile is chosen instead of the minimum in order to make the method more robust to sensor errors especially at far distances. Our method takes into account that in most indoor images captured by RGBD sensors, a part of the ground is visible. In order to account for cases where the ground is not visible, we discard scenes in which the majority of the normals from points on the hypothesized floor plane (first percentile) are not aligned with the upward direction.

HN-Label Generation: To transform depth into height, we calculate the distance between each 3D point and the floor plane. As for the normals, we compute the angle between every 3D point normal and the floor’s upward direction. We only use one angle to keep labels consistent over multiple viewpoints. Normals and heights are then binned, and we define our proposed alternative categories as all possible combinations of the normal and height bins. Figure 4 shows our proposed labels for the same scene from different viewpoints. Since we choose our labeling scheme to be view-independent, objects maintain the same labels throughout the scene recording.

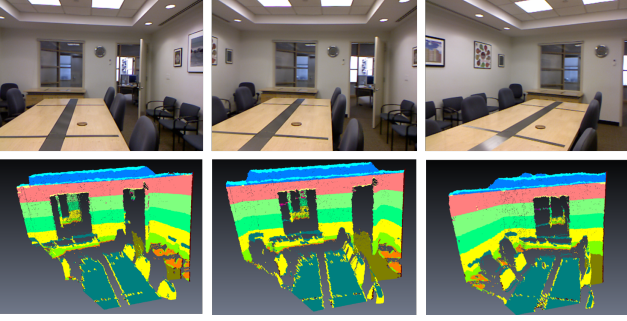


Figure 4. **HN-labels for different images in the same room.** Our proposed labels are view-independent and are consistent among different viewpoints.

3.3. Training with HN-Labels

Labels collected from height and normal information can be used to train the same network architecture used for semantic segmentation. Specifically, we choose the SegNet architecture [2] for this purpose, with an encoder network identical to the 13 convolutional layers in the VGG16 network [33], as well as, the DeepLabv3 architecture [6] with ResNetv2 layers [19]. Note that our method can be easily implemented with any other architecture and that the number of labels for semantic segmentation need not be similar to that of pre-training with HN-labels. In what follows, we will reference this trained network as the HN-network.

Once we train our HN-network with labels that are self-supervised, we need to transfer the representation to another network that learns to segment RGB images. In both the SegNet and DeepLabv3 architectures, the only difference between the two networks is the number of object classes, *i.e.* the number of outputs from the last convolution layer. Transfer learning can be done in two ways. The first way is to initialize all the layers of the semantic segmentation network with what was learned in the first network, and then finetune all the layers based on the manually labeled segmentation dataset. Another way of transfer learning is to keep some of the first layers unchanged, especially when the dataset used for pre-training is much larger than the dataset used for finetuning. This is motivated by the idea that generic information is usually shared at early layers.

Choosing to finetune only part of the network raises an important question: how many layers should be fixed and how many should be finetuned? Instead of manually selecting which layers to share and which layers to be task-specific, one can model the problem as a multi-task learning problem, in which sharing can be learned between the networks. This is mainly inspired by the work in [27]. Our joint network architecture, named cross-stitch [27], is shown in Figure 5. The shared representation part of the network is extracted from a network that was trained to out-

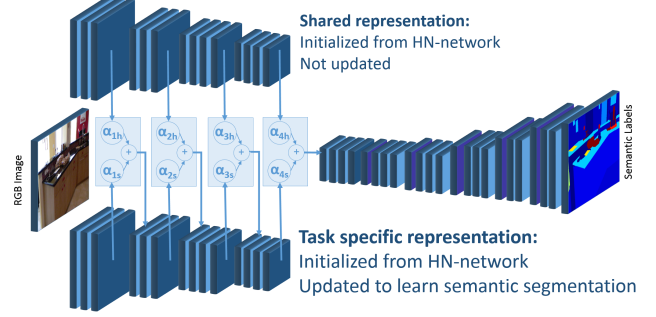


Figure 5. **Proposed fusion of HN-network and semantic segmentation network (Cross-Stitch).** The HN-network is considered as a shared representation whereas the semantic segmentation network is task specific. At every max-pooling layer, the network gets to choose between the pre-trained layers and the task specific layers.

put HN-labels, whereas the task-specific part learns to semantically segment. The shared representation part is kept fixed, reasoned by the large data that can be used to train that part. Sharing of layers is allowed at the first 4 max-pooling layers. We denote the output at every max-pooling by L_{xs} and L_{xh} , where x represents the index of the max-pooling layer. L_{xs} refers to the output generated in the “semantic segmentation network”, whereas L_{xh} refers to output from the HN-network. At every max-pooling layer, both representations are merged into

$$L = \alpha_{xh}L_{xh} + \alpha_{xs}L_{xs}$$

and L is used as an input to the subsequent layer of the semantic segmentation part of the network.

The final target is to achieve a higher accuracy in semantic segmentation only, especially when semantic labels are scarce. This differs from [27], which aims at achieving a better joint accuracy in multiple tasks.

Implementation Details: Our method is implemented using the Caffe framework [20] for the SegNet architecture and Tensorflow [1] for the DeepLabv3 architecture, both running on Titan X and Titan Xp GPUs. We use the same image input and output size for all of our networks. In the cases where depth sensors output a different size image, we compute the height on the original size image, then crop and reshape the color image with bilinear interpolation, while using nearest-neighbour interpolation for the labels. As for the training loss, we use the cross-entropy loss [26] in all our networks.

4. Experiments

4.1. Datasets

We generate our alternative label dataset from the unlabeled set of NYUv2 [28] dataset, which comprises more

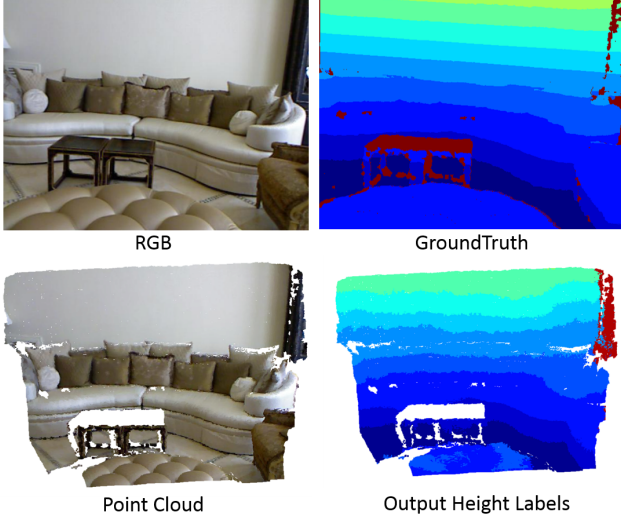


Figure 6. **Example of the output height labels obtained from the HN-network.** The labels are inpainted on the corresponding 3D point cloud. Groundtruth height labels are also shown.

Pre-training Method	Global acc	Avg acc	mIoU
no pre-training	38.74	13.73	8.78
height only	50.66	24.27	16.35
height 5 bins + normals	51.98	25.28	17.38
height 10 bins + normals	52.92	26.16	18.24

Table 2. **Ablation study.** This table shows the semantic segmentation network accuracy on NYUv2 when pre-trained from different versions of our proposed HN-network.

than 400K frames of indoor RGBD video sequences.

To evaluate the effect of our pre-training on semantic segmentation, we use the 1449 segmented frames of NYUv2 that are split into train and test, with the class label mapping coming from [15]. We also perform experiments on the Cambridge-driving Labeled Video Database (CamVid) [3], which contains scenes from the perspective of a driving automobile.

We use the following three conventional evaluation metrics: (i) global accuracy, (ii) class average accuracy, and (iii) mean intersection over union (IoU). Global accuracy is computed as the ratio between the number of correctly labeled pixels and the total number of pixels. The class average accuracy represents a scoring measure that weighs all classes similarly. The mean IoU also presents a measure that equally accounts for all classes and does not favor high accuracies in frequently occurring object classes.

4.2. Training the HN-Network

To train our proposed HN-network using the generated alternative labels, we use 41K frames from NYUv2 sampled uniformly from all scenes. We use a fixed $n_n = 2$ for

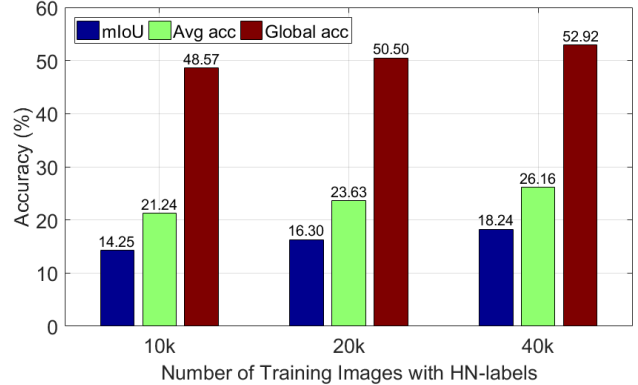


Figure 7. **Effect of dataset size.** Semantic segmentation network accuracy on NYUv2 increases when pre-trained from a larger number of training images with HN-labels.

normal bins, as indoor objects have surfaces that are mostly oriented either parallel or perpendicular to the floor plane. Our final label set contains $n_n \times n_h$ labels, with $n_h = 10$, and we discard points that do not have depth information. Also, we use the softmax cross-entropy loss during training that discards pixels with unknown depth label. For all experiments, the input image size is 424×560 , which enables us to only fit a batch of 4 images when training our HN-network. After 200K iterations in about 2 days, the training loss decreases to 4-5 times its initial value. We test our HN-network on NYUv2 test set. An example of the predicted height of the HN-network is shown in Figure 6 and compared to the groundtruth. Clearly, the network is able to learn and predict the correct height bin, which is an essential prior to using the same representation for semantic segmentation.

4.3. Training for Semantic Segmentation

We use the trained HN-network to initialize our second network for semantic segmentation on RGB images, as described in Section 3.3.

Ablation Studies: A comparison between different versions of our semantic segmentation method is presented in Table 2. We fix all the learning hyperparameters and run our experiment with SegNet architecture for 40K iterations (equivalent to about 50 epochs on the NYUv2 dataset). We compare our results against training from scratch with weight filler from [17]. Note that all measures are computed on 40 classes of NYUv2, which only contains 795 training images. Our network pre-trained with height labels achieved good performance, whereas adding the normal information boosted up the accuracy.

We also study the effect of training size on the final semantic segmentation accuracy in Figure 7. In this case, we fix the number of iterations for the HN-network and

Arch	Pre-training Method	Wall	Floor	Cabinet	Bed	Bookshelf	Sofa	Dresser	Avg acc	mIoU	Global acc
SegNet	No pre-training	77.57	74.91	42.36	13.25	6.58	22.42	3.17	13.73	8.78	38.74
	CIFAR100 pre-train	66.33	66.96	19.84	0.03	0.01	0.05	0	10.70	6.23	31.90
	ImageNet pre-train	81.54	86.1	58.86	37.76	35.05	38.25	4.35	25.40	17.34	50.58
	HN pre-training	83.26	90.63	58.81	58.40	38.79	37.05	14.24	26.16	18.24	52.92
DeepLab	No pre-training	18.70	66.72	60.78	22.30	20.70	15.24	12.49	24.77	6.73	31.41
	ImageNet pre-train	28.85	74.69	87.98	64.40	56.22	59.10	50.78	57.84	34.27	61.70
	HN pre-training	32.00	77.64	87.45	60.15	55.67	60.51	53.69	56.04	33.49	62.98

Table 3. **Evaluation of our proposed method.** The accuracy on some of the most occurring object labels in NUYv2 is shown, as well as the global and average accuracies on all 40 classes. Our method is compared to three baselines. The first one does not use additional labels to pre-train, whereas the second and third baselines use manually annotated labels for pre-training.

Method / Epoch	5	10	50	100
No pre-training	10.69	31.95	54.85	71.07
CIFAR100 pre-train	3.54	9.98	2.58	15.65
ImageNet pre-train	24.97	27.1	42.4	85.87
HN pre-training	78.98	81.70	84.5	86.03

Table 4. **Evaluation on the CamVid dataset using SegNet architecture.** The global accuracy is shown at different number of training epochs

semantic segmentation training. Our proposed method achieves good accuracy even with relatively small number of images with HN-labels. Higher accuracy is achieved with more training images, thus, exploiting the diversity among images in the larger set.

Semantic Segmentation Evaluation: Here, we compare our results to training from scratch, as well as, pre-training from the ImageNet and CIFAR100 [22] classification datasets. Semantic segmentation results on NYUv2 dataset are shown in Table 3 for both the SegNet architecture [2] and the DeepLabv3 architecture [6]. All finetuning experiments were done for 40K iterations (~ 50 epochs). If we compare the size of ImageNet to that of our alternative label dataset, ImageNet is about 25 times larger and requires more time to train. Nevertheless, initializing from our proposed dataset outperforms the ImageNet initialization for both architecture types. This shows that ability of our method to generalize to other architectures and backbones without requiring any expensive manual labelling. CIFAR100 initialization shows a degradation in accuracy over training from scratch (MSRA initialization [17]). This degradation is not unusual in the deep learning field, where training with atypical data would produce results closer to undesirable local minima.

Table 4 shows our experiments on the CamVid dataset using the SegNet architecture with VGG16 encoder, which contains images collected from outdoor settings. Initializ-

ing from the HN-labels dataset is still beneficial in such a setting, mainly due to the similarity in the task. The main intuition is that training on HN labels has learned to describe low-level feature information for the visual content in the image. Nonetheless, there exist differences in the high-level information between indoor and outdoor scenes, and this is noticeable in the relatively lower improvement for the outdoor scenes. Also, our method achieves the final accuracy much faster than other methods. This shows that although most objects in the outdoor setting were not previously seen by our pre-training network, it has still learned to discriminate between different patches.

Fixed Layers	ImageNet	Ours
conv1	50.1 / 25.1 / 16.9	54.1 / 27.9 / 19.7
conv1-conv2	51.5 / 25.3 / 17.5	54.0 / 27.8 / 19.6
conv1-conv3	51.5 / 25.3 / 17.4	52.9 / 26.9 / 18.7
conv1-conv4	50.8 / 25.4 / 17.5	54.4 / 28.1 / 19.4

Table 5. **Effect of fixing layers relative to finetuning all layers.**(Global acc/Avg acc/mIoU). Although ImageNet pre-training leads to better performance when some layers are fixed, our proposed method would always outperform it in the same setting.

We also try to initialize the segmentation network from our HN-network while keeping some layers intact. We finetune all other layers and stop at 40K iterations. The result on NYUv2 is shown in Table 5, which shows how global accuracy varies with fixing more layers. As can be seen, fixing up to four layers improves the final accuracy. This result can be reasoned because of the significant difference between the dataset used for pre-training and the one used for finetuning. Nevertheless, this observation cannot be used as a general conclusion as best accuracies can be achieved by fixing different number of layers in different scenarios. This motivates our next experiment, which learns what to share among layers between the two networks.

Cross-Stitching: We also conduct an experiment to fuse

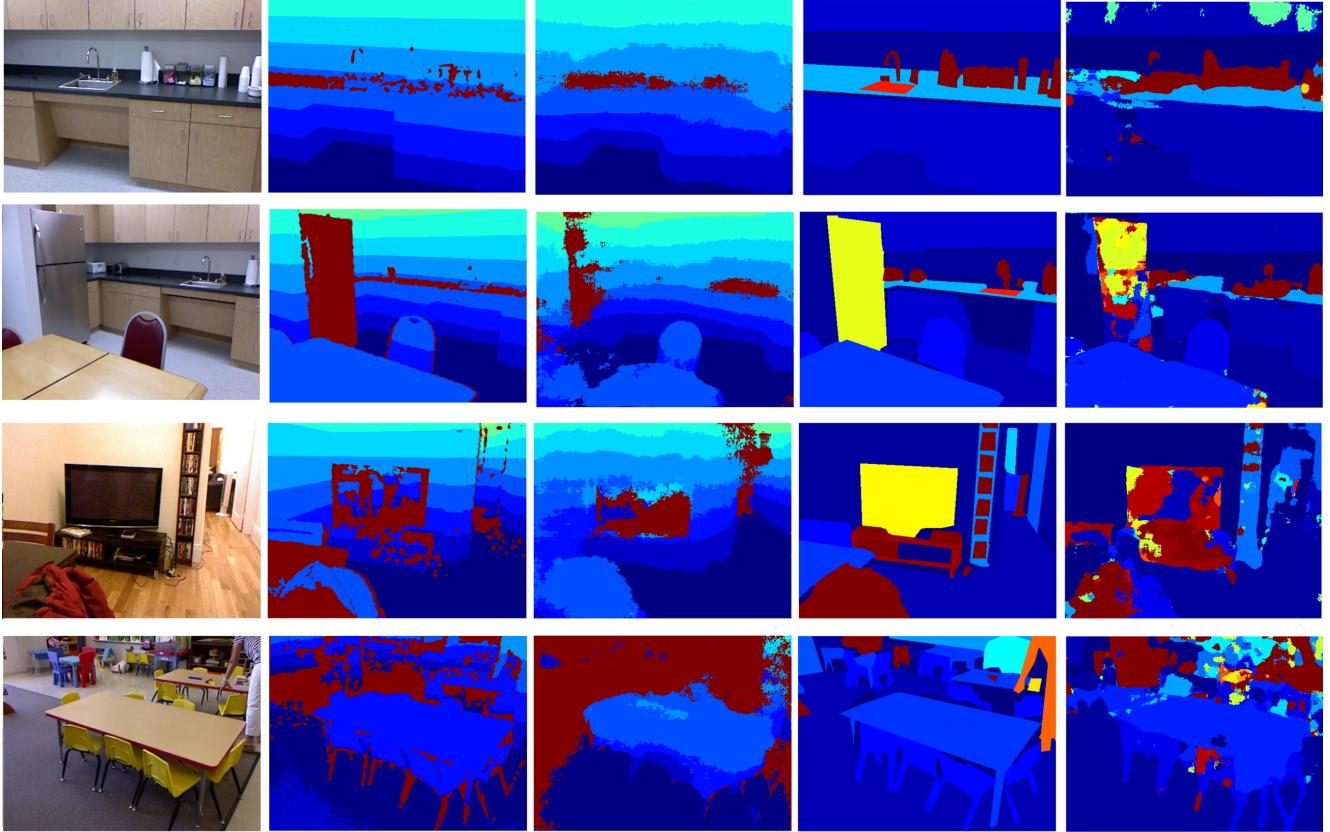


Figure 8. Qualitative evaluation of our proposed HN-network as well as the output of the semantic segmentation network. From left to right: Input RGB image, groundtruth height label, output height label, semantic groundtruth label, and output semantic label.

Method	Global acc	Avg acc	mIoU
ImageNet pre-training	50.58	25.40	17.34
ImageNet cross-stitch	50.94	25.33	17.35
Ours - No stitching	52.92	26.16	18.24
Ours cross-stitch	54.25	27.83	19.46

Table 6. **Evaluation of the cross-stitching result.** The cross-stitch result is compared against no stitching and ImageNet pre-training.

the HN-network with the semantic segmentation network. Instead of manually selecting the layers to share, our cross-stitch network learns to weigh the amount of sharing required between the two streams. The results are shown in Table 6, where we compare the final cross-stitched network to the non-stitched network and to the network pre-trained on ImageNet. We observe in our experiments that the final semantic segmentation accuracy increases without the need to manually select the number of layers to share and that cross-stitching is an essential component of its final performance. This represents a better way of transfer learning than basic initialization.

Qualitative Results: Figure 8 presents a set of RGB im-

ages from NYUv2 with their corresponding groundtruth height labels, predicted height labels from HN-network, along with the semantic groundtruth labels and the predicted semantic labels after cross-stitching. These images show that the current technique is capable of aptly generating semantic labels for RGB images along with height labels as a by-product. Also, the relation between the two tasks can be observed in areas like the ground, where a single height label corresponds to a single semantic label.

5. Conclusion

We present a novel method to pre-train any semantic segmentation network without the need for expensive manual labeling. Our pre-training learns from object heights, which are automatically extracted from depth sensors. Extensive experiments show that our proposed pre-training is better than initializing with ImageNet, while using much less data and without requiring any manual labels. We also propose to fuse the pre-training with the semantic segmentation network to better differentiate between task specific and shared representations, leading to higher overall accuracy. Since our pre-training does not require manual annotation, it is

easily scalable. Therefore, we suggest exploring such use of information to better improve the pre-training process to further improve performance over ImageNet pre-training.

References

- [1] Martín Abadi, Paul Barham, Jianmin Chen, Zhifeng Chen, Andy Davis, Jeffrey Dean, Matthieu Devin, Sanjay Ghemawat, Geoffrey Irving, Michael Isard, et al. Tensorflow: A system for large-scale machine learning. In *12th {USENIX} Symposium on Operating Systems Design and Implementation ({OSDI} 16)*, pages 265–283, 2016. 5
- [2] Vijay Badrinarayanan, Alex Kendall, and Roberto Cipolla. Segnet: A deep convolutional encoder-decoder architecture for image segmentation. *IEEE transactions on pattern analysis and machine intelligence*, 39(12):2481–2495, 2017. 2, 5, 7
- [3] Gabriel J Brostow, Julien Fauqueur, and Roberto Cipolla. Semantic object classes in video: A high-definition ground truth database. *Pattern Recognition Letters*, 30(2):88–97, 2009. 1, 6
- [4] Gabriel J Brostow, Julien Fauqueur, and Roberto Cipolla. Semantic object classes in video: A high-definition ground truth database. *Pattern Recognition Letters*, 30(2):88–97, 2009. 2
- [5] Liang-Chieh Chen, George Papandreou, Iasonas Kokkinos, Kevin Murphy, and Alan L Yuille. Deeplab: Semantic image segmentation with deep convolutional nets, atrous convolution, and fully connected crfs. *IEEE transactions on pattern analysis and machine intelligence*, 40(4):834–848, 2017. 2
- [6] Liang-Chieh Chen, George Papandreou, Florian Schroff, and Hartwig Adam. Rethinking atrous convolution for semantic image segmentation. *arXiv preprint arXiv:1706.05587*, 2017. 2, 5, 7
- [7] Marius Cordts, Mohamed Omran, Sebastian Ramos, Timo Rehfeld, Markus Enzweiler, Rodrigo Benenson, Uwe Franke, Stefan Roth, and Bernt Schiele. The cityscapes dataset for semantic urban scene understanding. In *Proceedings of the IEEE Conference on Computer Vision and Pattern Recognition*, pages 3213–3223, 2016. 2
- [8] Jia Deng, Wei Dong, Richard Socher, Li-Jia Li, Kai Li, and Li Fei-Fei. Imagenet: A large-scale hierarchical image database. In *Computer Vision and Pattern Recognition, 2009. CVPR 2009. IEEE Conference on*, pages 248–255. IEEE, 2009. 1, 3
- [9] David Eigen and Rob Fergus. Predicting depth, surface normals and semantic labels with a common multi-scale convolutional architecture. In *Proceedings of the IEEE International Conference on Computer Vision*, pages 2650–2658, 2015. 3
- [10] Mark Everingham, Luc Van Gool, Christopher KI Williams, John Winn, and Andrew Zisserman. The pascal visual object classes (voc) challenge. *International journal of computer vision*, 88(2):303–338, 2010. 2
- [11] Adrien Gaidon, Qiao Wang, Yohann Cabon, and Eleonora Vig. Virtual worlds as proxy for multi-object tracking analysis. In *Proceedings of the IEEE Conference on Computer Vision and Pattern Recognition*, pages 4340–4349, 2016. 3
- [12] Andreas Geiger, Philip Lenz, Christoph Stiller, and Raquel Urtasun. Vision meets robotics: The kitti dataset. *The International Journal of Robotics Research*, 32(11):1231–1237, 2013. 2
- [13] Bernard Ghanem, Ali Thabet, Juan Carlos Nibbles, and Fabian Caba Heilbron. Robust manhattan frame estimation from a single rgb-d image. In *Proceedings of the IEEE Conference on Computer Vision and Pattern Recognition*, pages 3772–3780, 2015. 4
- [14] Clément Godard, Oisin Mac Aodha, and Gabriel J Brostow. Unsupervised monocular depth estimation with left-right consistency. In *Proceedings of the IEEE Conference on Computer Vision and Pattern Recognition*, pages 270–279, 2017. 3
- [15] Saurabh Gupta, Pablo Arbelaez, and Jitendra Malik. Perceptual organization and recognition of indoor scenes from rgb-d images. In *Proceedings of the IEEE Conference on Computer Vision and Pattern Recognition*, pages 564–571, 2013. 6
- [16] Saurabh Gupta, Ross Girshick, Pablo Arbeláez, and Jitendra Malik. Learning rich features from rgb-d images for object detection and segmentation. In *European Conference on Computer Vision*, pages 345–360. Springer, 2014. 3
- [17] Kaiming He, Xiangyu Zhang, Shaoqing Ren, and Jian Sun. Delving deep into rectifiers: Surpassing human-level performance on imagenet classification. In *Proceedings of the IEEE international conference on computer vision*, pages 1026–1034, 2015. 6, 7
- [18] Kaiming He, Xiangyu Zhang, Shaoqing Ren, and Jian Sun. Deep residual learning for image recognition. In *Proceedings of the IEEE conference on computer vision and pattern recognition*, pages 770–778, 2016. 2
- [19] Kaiming He, Xiangyu Zhang, Shaoqing Ren, and Jian Sun. Identity mappings in deep residual networks. In *European conference on computer vision*, pages 630–645. Springer, 2016. 5
- [20] Yangqing Jia, Evan Shelhamer, Jeff Donahue, Sergey Karayev, Jonathan Long, Ross Girshick, Sergio Guadarrama, and Trevor Darrell. Caffe: Convolutional architecture for fast feature embedding. In *Proceedings of the 22nd ACM international conference on Multimedia*, pages 675–678. ACM, 2014. 5
- [21] Alex Kendall, Yarin Gal, and Roberto Cipolla. Multi-task learning using uncertainty to weigh losses for scene geometry and semantics. In *Proceedings of the IEEE Conference on Computer Vision and Pattern Recognition*, pages 7482–7491, 2018. 3
- [22] Alex Krizhevsky and Geoffrey Hinton. Learning multiple layers of features from tiny images. Technical report, Cite-seer, 2009. 7
- [23] Alex Krizhevsky, Ilya Sutskever, and Geoffrey E Hinton. Imagenet classification with deep convolutional neural networks. In F. Pereira, C. J. C. Burges, L. Bottou, and K. Q. Weinberger, editors, *Advances in Neural Information Processing Systems 25*, pages 1097–1105. Curran Associates, Inc., 2012. 2
- [24] Gustav Larsson, Michael Maire, and Gregory Shakhnarovich. Colorization as a proxy task for visual

- understanding. In *Proceedings of the IEEE Conference on Computer Vision and Pattern Recognition*, pages 6874–6883, 2017. 3
- [25] Tsung-Yi Lin, Michael Maire, Serge Belongie, James Hays, Pietro Perona, Deva Ramanan, Piotr Dollár, and C Lawrence Zitnick. Microsoft coco: Common objects in context. In *European conference on computer vision*, pages 740–755. Springer, 2014. 2
- [26] Jonathan Long, Evan Shelhamer, and Trevor Darrell. Fully convolutional networks for semantic segmentation. In *Proceedings of the IEEE Conference on Computer Vision and Pattern Recognition*, pages 3431–3440, 2015. 2, 5
- [27] Ishan Misra, Abhinav Shrivastava, Abhinav Gupta, and Martial Hebert. Cross-stitch networks for multi-task learning. In *Proceedings of the IEEE Conference on Computer Vision and Pattern Recognition*, pages 3994–4003, 2016. 3, 5
- [28] Pushmeet Kohli Nathan Silberman, Derek Hoiem and Rob Fergus. Indoor segmentation and support inference from rgb-d images. In *ECCV*, 2012. 1, 3, 4, 5
- [29] Mehdi Noroozi and Paolo Favaro. Unsupervised learning of visual representations by solving jigsaw puzzles. In *European Conference on Computer Vision*, pages 69–84. Springer, 2016. 3
- [30] German Ros, Laura Sellart, Joanna Materzynska, David Vazquez, and Antonio M Lopez. The synthia dataset: A large collection of synthetic images for semantic segmentation of urban scenes. In *Proceedings of the IEEE Conference on Computer Vision and Pattern Recognition*, pages 3234–3243, 2016. 3
- [31] Guy Rosman, Xue-Cheng Tai, Ron Kimmel, and Alfred M Bruckstein. Augmented-lagrangian regularization of matrix-valued maps. *Methods and Applications of Analysis*, 21(1):121–138, 2014. 4
- [32] Ali Sharif Razavian, Hossein Azizpour, Josephine Sullivan, and Stefan Carlsson. Cnn features off-the-shelf: an astounding baseline for recognition. In *Proceedings of the IEEE conference on computer vision and pattern recognition workshops*, pages 806–813, 2014. 3
- [33] K. Simonyan and A. Zisserman. Very deep convolutional networks for large-scale image recognition. *CoRR*, abs/1409.1556, 2014. 2, 5
- [34] Shuran Song, Samuel P Lichtenberg, and Jianxiong Xiao. Sun rgb-d: A rgb-d scene understanding benchmark suite. In *Proceedings of the IEEE conference on computer vision and pattern recognition*, pages 567–576, 2015. 3
- [35] Christian Szegedy, Wei Liu, Yangqing Jia, Pierre Sermanet, Scott Reed, Dragomir Anguelov, Dumitru Erhan, Vincent Vanhoucke, and Andrew Rabinovich. Going deeper with convolutions. In *Computer Vision and Pattern Recognition (CVPR)*, 2015. 2
- [36] Sudheendra Vijayanarasimhan, Susanna Ricco, Cordelia Schmid, Rahul Sukthankar, and Katerina Fragkiadaki. Sfmnet: Learning of structure and motion from video. *arXiv preprint arXiv:1704.07804*, 2017. 3
- [37] Fisher Yu and Vladlen Koltun. Multi-scale context aggregation by dilated convolutions. In *ICLR*, 2016. 2
- [38] Andy Zeng, Kuan-Ting Yu, Shuran Song, Daniel Suo, Ed Walker, Alberto Rodriguez, and Jianxiong Xiao. Multi-view self-supervised deep learning for 6d pose estimation in the amazon picking challenge. In *Robotics and Automation (ICRA), 2017 IEEE International Conference on*, pages 1386–1383. IEEE, 2017. 3
- [39] Hengshuang Zhao, Jianping Shi, Xiaojuan Qi, Xiaogang Wang, and Jiaya Jia. Pyramid scene parsing network. In *Proceedings of the IEEE conference on computer vision and pattern recognition*, pages 2881–2890, 2017. 2
- [40] Tinghui Zhou, Matthew Brown, Noah Snavely, and David G Lowe. Unsupervised learning of depth and ego-motion from video. In *Proceedings of the IEEE Conference on Computer Vision and Pattern Recognition*, pages 1851–1858, 2017. 3